1-1-2015

Superior critical current density obtained in Mg11B2 low activation superconductor by using reactive amorphous 11B and optimizing sintering temperature

Fang Cheng
Tianjin University

Yongchang Liu
Tianjin University, Nankai University

Zongqing Ma
University of Wollongong, zqma@uow.edu.au

Huijun Li
Tianjin University

Md Shahriar Hossain
University of Wollongong, shahriar@uow.edu.au

Superior critical current density obtained in Mg11B2 low activation superconductor by using reactive amorphous 11B and optimizing sintering temperature

Abstract

The un-doped $Mg^{11}B2$ and Cu-doped $Mg^{11}B2$ bulks using ^{11}B as a boron precursor were fabricated by solid-state reaction and sintered at different temperature in present work. By analyzing the sintering process, it was found that ^{11}B original powder is more reactive and can react with Mg severely even at low temperature before Mg melting, which leads to the formation of refined $Mg^{11}B2$ grains. Consequently, the critical current density of $Mg^{11}B2$ sample prepared in this work is higher than that of natural MgB2. Furthermore, it was found that proper Cu addition could obviously accelerate the reaction between Mg and ^{11}B and promote the formation of $Mg^{11}B2$ due to the appearance of Mg-Cu liquid at low sintering temperature before Mg melting. On the other hand, Cu addition also introduced more $MgCu_2$impurity, leading to a relatively lower critical current density on the whole. Interestingly, the critical current density of the Cu doped sample sintered at 800 °C is surprisingly enhanced at the low field, compared with that of the corresponding un-doped one. This is due to the peritectic reaction which generated small-sized $MgCu_2$ occurred that at 800 °C, providing $MgCu_2$ pinning centers well-distributed in the MgB2 matrix.

Keywords

low, temperature, sintering, obtained, density, current, critical, superior, optimizing, amorphous, reactive, superconductor, activation, 11b, mg11b2

Disciplines

Engineering | Physical Sciences and Mathematics

Publication Details

Cheng, F., Liu, Y., Ma, Z., Li, H. & Hossain, M. Al. (2015). Superior critical current density obtained in $Mg^{11}B_2$ low activation superconductor by using reactive amorphous ^{11}B and optimizing sintering temperature. Journal of Alloys and Compounds, 650 508-513.

Superior critical current density obtained in $Mg^{11}B_2$ low activation superconductor by using reactive amorphous ^{11}B and optimizing sintering temperature

Fang Cheng[1], Yongchang Liu[1], Zongqing Ma[1, 2*], Huijun Li[1], M. Shahriar Al Hossain[2]

1. *Tianjin Key Laboratory of Composite and Functional Materials, School of Materials Science & Engineering, Tianjin University, Tianjin 300072, People's Republic of China*
2. *Institute for Superconducting and Electronic Materials, University of Wollongong*

Abstract

The un-doped $Mg^{11}B_2$ and Cu-doped $Mg^{11}B_2$ bulks using ^{11}B as a boron precursor were fabricated by solid-state reaction and sintered at different temperature in present work. By analyzing the sintering process, it was found that ^{11}B original powder is more reactive and can react with Mg severely even at low temperature before Mg melting, which leads to the formation of refined $Mg^{11}B_2$ grains. Consequently, the critical current density of $Mg^{11}B_2$ sample prepared in this work is higher than that of natural MgB_2. Furthermore, it was found that proper Cu addition could obviously accelerate the reaction between Mg and ^{11}B and promote the formation of $Mg^{11}B_2$ due to the appearance of Mg-Cu liquid at low sintering temperature before Mg melting. On the other hand, Cu addition also introduced more $MgCu_2$impurity, leading to a relatively lower critical current density on the whole. Interestingly, the critical current density of the Cu doped sample sintered at 800 ^oC is surprisingly enhanced at the low field, compared with that of the corresponding un-doped one. This is due to the peritectic reaction which generated small-sized $MgCu_2$ occurred that at 800 ^oC, providing $MgCu_2$ pinning centers well-distributed in the MgB_2 matrix.

Keywords: MgB_2 superconductor; isotope; Cu doping; Critical current density.

* Corresponding author Tel & Fax: 0086-22-87401873 E-mail: mzq0320@163.com

1. Introduction

The superconductivity of MgB_2 below 39 K has been discovered and widely investigated since 2001[1]. MgB_2 attracted lots of attention because of its simple crystal structure, large coherence length, relatively high critical current density, and transparency of the grain boundaries. During the development for more than 10 years, MgB_2 has been fabricated[2-10]into bulks, single crystals, thin films, tapes and wires. Such basic properties and preparation techniques allow MgB_2 to be apromising material for both large-scale applications and electronic devices. Controllable thermonuclear fusion is the ultimate ideal of mankind energy. Using high temperature magnetic field constraint of Tokamak plasma is considered to be the most likely device to realize the controlled thermonuclear fusion reaction[11]. Nowadays the applied of Nb-based superconducting wires, the decay time of induced radioactivity takes too long, and it costs much time to cool down. The long decay time brings awful effects in environment and radiation-processing reactor which definitely increase the difficulty of construction and the cost. Compared with Nb-based superconductor, MgB_2 have advantage in decay time which is much shorter and properties. From the comparing above, we can obtain that MgB_2 superconducting wires has a great application prospect in the fusion reactor. To be an appropriate material for the superconducting wire using in the future, one must consider the influence caused by neutron irradiation induced radioactivity and superconducting performance degradation in the design of superconducting magnet coils. Natural elementary boron is commonly composed of 20% ^{10}B and 80% ^{11}B. The former played an important role in the industry because of the large thermal neutron capture cross section, which issued as the reactor neutron absorber or shielding material. However, for the MgB_2 wires synthesized from natural elementary boron, ^{10}B will be consumed in the

irradiation environment according to the reaction $^{10}B + n \rightarrow {}^{7}Li + He$ (gas),which will lead to partial destruction of the MgB_2 wire, and as a result, there is no guarantee for the long-term stability of the MgB_2 superconducting magnet. Isotope research shows that^{11}B is much more stable than ^{10}B in neutron irradiation environment due to the smaller neutron capture cross section [12]. In order to ensure the operation stability of MgB_2 superconductor magnet, and to avoid the reduction of the superconductor volume fraction, the isotope ^{11}B becomes a possible substitute for nature B. The previous studies focused on the theoretical calculation [14-15] more and the experiment research much less. The previous experimental studies put many emphases on the performance of the $Mg^{11}B_2$ superconducting wires[16-17], which showed obvious differences in contrast with the traditional MgB_2 wire, and the critical current density exhibits lower than the traditional MgB_2 [17]. Few studies have addressed on the sintering mechanism, transporting properties and neutron irradiation impacting of the $Mg^{11}B_2$ wires, and a further research is required.

For this reason, the research of the sintering mechanism and improving the critical current density has been discussed in present study. In this study pure ^{11}B was used as the raw material instead of natural B, with the purpose of solving the Tokamak plasma problem in controllable thermonuclear fusion. Besides the un-doped samples, we also investigated the sintering process and the phase formation for Cu-doped samples through thermal analysis, phase identification and microstructure observation. Combined with the measurement of the critical current density, the effects of the element ^{11}B are concluded.

2. Experimental details

The samples of un-doped $Mg^{11}B_2$ and $Mg^{11}B$+5wt.% Cu were prepared by a solid-state sintering method. ^{11}B powders (Amorphous, 99.2% in purity, about 5μm in

size, from Pavezyum Kimya, Turkey), natural B powder (Amorphous, 99% in purity, 25 μm in size), Mg powders (99.5% in purity, 100 μm in size, Fuchen Chemical Reagent Company), and Cu powders (99.7% in purity, 3 μm in size, Aladdin Chemical Reagent Company) were separately mixed in the ratio of $Mg^{11}B_2$ and $Mg^{11}B_2$+5wt% Cu. Then, the mixed powders were pressed into cylindrical pellets (Φ5×1.5mm). All the un-doped and Cu-doped samples were sintered in differential thermal analysis (Mettler Toledo TGA/DSC1/) at 750^{o}C, 800^{o}C, and 850^{o}C for 45 minutes under flowing high-purity Ar gas with a heating rate of 10^{o}C min^{-1} and then cooled down to room temperature with a heating rate of -40^{o}C min^{-1}.The phase composition of the sintered samples was examined by X-ray diffractometer (XRD, Rigaku D/max 2500) using Cu Kα radiation, and the morphology of the samples was characterized by scanning electron microscope (SEM, S-4800, Hitachi) and transmission electron microscope (TEM, JSM-2100, Hitachi). The superconducting properties were measured by superconducting quantum interference device (SQUID VSM, Quantum Design), after the samples were cut into a slab of size about 4×2×1 mm^3. The corresponding J_c values were calculated from the width of magnetization hysteresis loops based on the Bean model J_c=20ΔM/[a/(1-a/3b)][18], where ΔM is the volume magnetization, and a and b are the sample dimensions.

3. Results and discussion

To acquire thermodynamics for the entire sintering process, the recorded DSC curves for the un-doped and Cu-doped $Mg^{11}B_2$ samples during the heating stage are shown in Fig. 1. The reference MgB_2 is prepared using natural boron powder. Three peaks are recognized from the curves, and they are in sequence corresponded to

solid-solid reaction of Mg and B, Mg melting, and Mg-B liquid-solid reaction. By comparing the curves of the un-doped samples, it is found that the height of the two exothermic peaks is different. Meaningfully, the solid-solid reaction for the $Mg^{11}B_2$ became more intense than that for the referred normal MgB_2, which means that ^{11}B powder used here is more reactive than natural B, so that the reaction between Mg and ^{11}B almost had completed in solid-solid reaction, there is only very little residual Mg and ^{11}B continue in liquid-solid reaction. In previous study, it can be discovered that Cu addition [19-20] could promote the reaction between Mg and B. Hence, the study would be valuable in order to clarify whether could promote the sintering of Mg and ^{11}B. From the DSC curve of the Cu-doped $Mg^{11}B_2$ sample, the endothermic peak of Mg melting becomes weak, and the peak indicating liquid-solid reaction gets lower. The two exothermic stages are continuous rather than be separated by the Mg melting. Due to the eutectic reaction between Mg and Cu at 485^{o}C, the solid-solid reaction of the Cu-doped $Mg^{11}B_2$ sample started earlier than the un-doped sample. This result indicates that the Mg-Cu eutectic liquid is definitely effective to accelerate the reaction between Mg and ^{11}B to some extent.

The X-ray diffraction patterns of the un-doped $Mg^{11}B_2$ and Cu-doped $Mg^{11}B_2$ samples are represented in Fig.2. One can see that the superconducting phase MgB_2 and the impurity phase MgO exist in all the sintered samples, and $MgCu_2$ appeared as the second impurity phase in Cu-doped samples. Both the un-doped and the Cu-doped samples were sintered at 750-850 ^{o}C. It is also observed that the intensity of MgB_2 peaks increased with the increasing sintering temperature for the un-doped samples, indicating the improvement of the crystallinity. For the Cu-doped samples, higher sintering temperature also brought about stronger peak intensity, but the sample sintered at 800^{o}C shows anomalously better crystallinity than the sample sintered at

850^{o}C which the reason will be discussed in the following part. The full width at half maximum (FWHM) calculated from the XRD could also gave a clue of the degree of the crystallization.

Figure 3 shows the FWHM values of the (101), (002) and (111) characteristic peaks for the un-doped and Cu-doped samples sintered at different temperatures. No variation tendency for the un-doped samples is observed, and the Cu doping resulted in either decrease of the FWHM value or few changes at 750^{o}C and 850^{o}C. The Cu-doped sample sintered at 800^{o}C showed increased FWHM value in contrast with the un-doped sample, which is in agreement with the anomaly of the XRD pattern. The increase of FWHM indicates the decrease of the grain size as well as the crystallinity. The lattice parameters of sintered samples were also calculated based on the XRD data and shown in Table 1. It was found that the lattice parameters of Cu-doped samples are comparable to that of the un-doped samples within the calculation error, which suggests that the minor Cu addition mainly reacted with Mg forming the Mg-Cu alloys, not substitute for Mg in the MgB2 crystal lattice [21].

The volume fraction of impurities including MgO in the samples is calculated from the XRD patterns, as shown in Fig.4. For the un-doped samples, the volume fraction of MgO exhibits an increasing trend with the increasing temperature, and becomes stable finally. The fraction of the Cu-containing impurity remained unchanged when the sintering temperature increased as the doped Cu content was the same.

From the whole variation tendency for all the samples, we can obtain that the MgO content of Cu-doped sample is higher than un-doped one at the same sintering temperature, and one could indeed find this for the samples sintered at 750 ^{o}C and 850 ^{o}C from Fig. 4. Considering the mentioned eutectic liquid, the MgO content in the Cu-doped samples is supposed to be higher than that in the un-doped samples due to

the Mg-Cu eutectic liquid active the reaction, but another anomaly appeared for the Cu-doped sample sintered at 800 ^{o}C that the MgO content reduced compared with the un-doped sample. The phase diagram [22] provides a hint for this special phenomenon that the temperature for the peritectic reaction Mg-Cu(l)+$MgCu_2$(s)→Mg_2Cu(s) is around 800^{o}C, and the reaction 3Mg_2Cu+6B→3MgB_2+$MgCu_2$ would subsequently occur. As a result, the reactions work as a loop during the holding process. The generated $MgCu_2$ accelerated the consumption of the Mg-Cu liquid in return, which hindered the oxidation of the Mg-Cu liquid as well. Nevertheless, the content of the impurity phase for the Cu-doped samples is over 20%, which might be harmful to the J_c performance.

The microstructure of the un-doped and the Cu-doped samples, especially the form of the impurities, can be observed from the SEM images, as shown in Fig.5. On the whole, the samples are of good grain connectivity, and the recognized regular $Mg^{11}B_2$ grains with an average size of about 600-800nm. The white and bright particles with an average size of about 50-100nm are MgO impurities, existing among the grains in the un-doped samples (see Fig. 5a-5c), and the distribution and the size of the impurity decreased with the increasing temperature. For the Cu-doped samples, small-sized impurity particles are dispersed on the MgB_2 matrix besides the existence of MgO. The white and bright particles should be MgO or $MgCu_2$ with an average size of about 30-50nm (see Fig. 5e-5f). The size and amount of the impurity decreased first and then increased because of the special point of 800 ^{o}C (as we had explained about Fig.4). During the holding process, the equilibrium between Mg-Cu(l) and Mg(s) encouraged the dissociative Mg(s) underwent a partial dissolution and precipitation to become more active and more easy to react with B. If the holding time is long enough, the reactions will continue until B is completely consumed. One can observe that the

second exothermic peak of un-doped sample is higher than the Cu-doped sample due to the process of dissolution and precipitation of un-doped $Mg^{11}B_2$, but the solid-liquid reaction is not intense enough. Therefore, the process of dissolution and precipitation that improves the crystallinity in the Cu-doped sample could not proceed as completely as that for the un-doped sample. It as a result led to the low crystallinity of the Cu-doped sample sintered at 850 ^{o}C.

The HRTEM image for the Cu-doped sample sintered at 800^{o}C is shown in Fig. 6. Two grains of MgB_2 were recognized with 20-nm black second-phase particles (indicated as MgO or $MgCu_2$) distributing in the matrix, and the size is consistent with that of the fine particles observed in the SEM image. This size allows these particles to be effective pinning centers, whereas that of the agminate impurity in the top left corner is in agreement with the MgO dimension in the SEM images.

Figure 7 shows the temperature dependence of magnetization curves for the un-doped and Cu-doped $Mg^{11}B_2$ samples, and the value of T_c and ΔT have been shown in Table 1 which is easy to compare. The critical temperature of un-doped and Cu-doped samples is lower than the normal MgB_2 due to the isotope effect of superconductor. Though not obviously, the critical temperature of all the samples is above 35K which still meets the actual needs of practical applications. Thereinto, the Cu-doped sample sintered at 800^{o}C showed the T_c abnormally higher than the others, which should be attributed to the high-quality MgB_2 generated from the peritectic reaction. Besides, the transition width, ΔT, which means the interval between $T_{c,\,onset}$ and $T_{c,\,end}$, decreased with the increasing sintering temperature. The high critical temperature and sharp transition width indicate that the samples are of high crystallinity and homogeneity. It is suggested that the generated Mg-Cu(l) increased the uniformity of Cu-doped samples. As far as the Cu-doped samples sintered at

800^{o}C, the highest T_c and the sharpest transition is mostly due to that peritectic reaction promoted Cu element to distribute homogeneously.

The critical current density (J_c) and the irreversible field (H_{irr}) of samples is illustrated in Fig.8 and Table 1. H_{irr} is value of H when J_c is equal to 100 A cm^{-2}. For the un-doped samples, the values of H_{irr} are increasing as the sintering temperature increasing. As for the Cu-doped samples, the values of H_{irr} are increasing first and then decreasing with the sintering temperature increasing. Compared with the reference MgB_2 [20], the J_c of all the un-doped $Mg^{11}B_2$ samples was enhanced over the entire field. The solid-solid reaction of Mg-^{11}B is more drastic than Mg-B because of the higher reactivity of ^{11}B. Fine MgB_2 grains are caused by the intense solid-solid reaction along with poor crystallinity. As a result, more grain-boundary pinning is induced, and the J_c is improved. The samples with Cu addition showed relatively lower J_c than the un-doped samples because Cu addition generated more impurity phase, which led to less superconducting phase [24] and weaker connectivity among the grains. However, it is noticed that the Cu-doped sample sintered at 800^{o}C exhibited higher J_c than the un-doped one sintered at the same temperature, owing to the peritectic reaction that brought homogeneously distributed impurity. From the results above, it is referred that slightly Cu addition has positive effects on the crystallinity and homogeneity, and 800 ^{o}C is an appropriate sintering temperature for improving the low-field J_c for the $Mg^{11}B_2$ samples.

4. Conclusions

In summary, we had synthesized the un-doped $Mg^{11}B_2$ and Cu-doped $Mg^{11}B_2$ samples. The solid-solid reaction of $Mg^{11}B_2$ is more drastic than traditional MgB_2 because of the higher reactivity of ^{11}B, which results in the enhancement of J_c in the $Mg^{11}B_2$ samples. Generally, Cu addition introduced a high content of impurity,

leading to a lower critical current density than the un-doped $Mg^{11}B_2$ samples. But the Cu-doped sample sintered at 800 ^{o}C in present work showed higher J_c performance at low field, in contrast with the un-doped sample sintered at the same temperature, due to the peritectic reaction occurred at 800 ^{o}C.

Acknowledgement *This work is supported by the Australian Research Council (Grant No. DE140101333) and internal grants by the University of Wollongong (UOW) e University Research Council (URC) and Australian Institute for Innovative Materials (AIIM) in 2014-15.The authors are grateful to China National Funds for Distinguished Young Scientists (Grant No. 51325401), the National Natural Science Foundation of China (Grant No. 51302186), the Natural Science Foundation of Tianjin (Grant No. 13JCZDJC32300 and 14JCQNJC03300). We also thank Pavezyum Kimya for providing high quality amorphous 11B powders.*

References:

[1] Nagamatsu N, Nakagawa N, Muranaka T, Zenitani Y, Akimitsu J. Superconductivity at 39 K in magnesium diboride. Nature 2001; (410):63–64.

[2] Lu J, Xiao Z, Lin Q, Claus H, Fang ZZ. Low-temperature synthesis of superconducting nanocrystalline MgB_2. J.Nanomater. 2010; (2010): 191058.

[3] Nath M, Parkinson BA. A simple sol-gel synthesis of superconducting MgB_2 nanowires. Adv. Mater. 2006; (18):1865-1868.

[4] Jha AK, Khare N. Single-crystalline superconducting MgB_2 nanowires. Supercond.Sci. Technol. 2009;(22):075017.

[5] Fujii H, Ozawa K. Critical temperature and carbon substitution in MgB_2 prepared through the decomposition of $Mg(BH_4)_2$. Supercond. Sci. Technol. 2010;(23):125012.

[6] Chen LP, Zhang C, Wang YB, Wang Y, Feng QR, Gan ZZ, Yang JZ, Li XG.A sol–gel method for growing superconducting MgB_2films.Supercond. Sci. Technol.

2011;(24):015002.

[7] Kang WN, Kim HJ, Choi EH, Jung CU, Lee SI.MgB_2 superconducting thin films with a transition temperature of 39 Kelvin. Science 2001;(292):1521-1523.

[8] Hossain MSA, Senatore C, Flukiger R, Rindfleisch MA, Tomsic MJ, Kim JH, Dou SX. The enhanced J_c and B_{irr} of in situ MgB_2 wires and tapes alloyed with $C_4H_6O_5$ (malic acid) after cold high pressure densification.Supercond. Sci. Technol. 2009;(22):095004.

[9] Li GZ, Yang Y, Susner MA, Sumption MD, Collings EW. Critical current densities and *n*-values of MgB_2 strands over a wide range of temperatures and fields. Supercond. Sci. Technol. 2012;(25):025001.

[10] Kim JH, Oh S, Kumakura H, Matsumoto A, Heo YU, Song KS, Kang YM, Maeda M, Rindfleisch M, Tomsic M, Choi S, Dou SX. Tailored materials for high-performance MgB_2 wire. Adv. Mater. 2011;(23):4942-4946.

[11] Chen FF. Introduction to plasma physics and controlled fusion. NewYork Plenum press. 2010.

[12] Mooring EP, Monahan JE, Huddleston CM. Neutron cross sections of the boron isotopes for energies between 10 and 500 keV. Nucl. Phys. 1966; (82):16.

[13] Bud'ko SL, Lapertot G, PetrovicC, Cunningham CE, Anderson N, Canfield PC. Boron isotope effect in superconducting MgB_2. Phys. Rev. Lett. 2001; (86):1877-1880.

[14] Hinks D G, JorgensenJD. The isotope effect and phonons in MgB_2. Physica C.2003; (385):98-104.

[15] Choi HJ,Cohen ML, Louie SG. Anisotropic Eliashberg theory of MgB_2: Tc, isotope effects,superconducting energy gaps, quasiparticles, and specific heat. Physica C.2003; (385): 66-74.

[16] Pitt MP, Webb CJ, Paskevicius M, Sheptyakov D, Buckley CE, Gray EM. In situ neutron diffraction study of the deuteration of isotopic $Mg^{11}B_2$. J. Phys. Chem. C. 2011;(115):22669–22679.

[17] Hishinumaa Y, Kikuchib A, Matsudac K, Nishimurac K, Kubotad Y, Hatad S, Yamadaa S, Takeuchib T. Microstructure and superconducting properties of Cu addition MgB_2 multifilamentary wires using boron isotope powder as the boron source material. Phys. Procedia. 2012;(36):1486-1491.

[18] Bean CP. Magnetization of high-field superconductors. Phys. Rev. Lett. 1962;(8):250.

[19] Ma ZQ, Liu YC, Shi QZ, Zhao Q, Gao AM. The mechanism of accelerated phase formation of MgB_2 by Cu-doping during low-temperature sintering. Materials Research Bulletin. 2009; (44): 531-537.

[20] Ma ZQ, Liu YC, Han YJ, Zhao Q, Gao AM. Variation of the enhancement mechanism in the critical current density of Cu-doped MgB_2 samples sintered at different temperatures. J. Appl. Phys. 2008; (104):063917.

[21] Ma ZQ, Liu YC, Shi QZ, Zhao Q, Gao ZM. The improved superconductive properties of MgB_2 bulks with minor Cu addition through reducing the MgO impurity. Physica C. 2008; (468): 2250–2253.

[22] The Materials Information Society, Binary alloy phase diagram 2nd edn plus updates, 1996, (Metal Park, OH: ASM International).

[23] Shi QZ, Liu YC, Gao ZM, Zhao Q, Ma ZQ. Phase formation process of bulk MgB_2 analyzed by differential thermal analysis during sintering. J. Alloy. Compd. 2008;(458): 553–557.

[24] HishinumaY, Kikuchi A, Iijima Y, Yoshida Y, Takeuchi T, Nishimura T. Fabrication of MgB_2 superconducting wires as low activation superconducting

materials for an advanced fusion reactor application. Fusion Eng. Des. 2006; (81): 2467-2471.

Table 1. The structural and superconducting parameters of the samples

Sample		a(Å)	c(Å)	T_c(K)	ΔT (K)	H_{irr} (T)	J_c at 3T ($\times 10^3$A·cm^{-2})
Un-doped	750^{o}C	3.08202	3.52114	36.7	0.6400	4.56	4.337
	800^{o}C	3.07695	3.52126	36.3	0.3883	4.63	4.067
	850^{o}C	3.08116	3.52169	36.8	0.3905	4.82	6.538
Cu-doped	750^{o}C	3.05278	3.52150	36.3	0.3833	4.09	2.331
	800^{o}C	3.08026	3.52121	36.7	0.4216	4.26	2.266
	850^{o}C	3.08036	3.52350	36.5	0.4595	3.67	0.869

Figure captions

Fig. 1 Measured DSC curvesduring the sintering of un-doped and Cu-doped. $Mg^{11}B$ samples with an applied heating rate of 10^{o}C/min. The reference MgB_2[23] is made from the normal boron.

Fig. 2 The XRD patterns of samples sintered at 750^{o}C, 800 ^{o}C, 850 ^{o}C for 45 min (a) un-doped $Mg^{11}B_2$ and (b) Cu-doped $Mg^{11}B_2$ samples.

Fig. 3 Full width at half maximum ofthe (101), (002), and (111) peaks for the un-doped and Cu-doped $Mg^{11}B_2$ samples.

Fig. 4 Volume fraction of the impurities for un-doped and Cu-doped $Mg^{11}B_2$ samples sintered at 750-850 ^{o}C.

Fig. 5 SEM images for the un-doped sintered at (a) 750^{o}C, (b) 800^{o}C, (c) 850^{o}C,and the Cu-doped $Mg^{11}B_2$ samples sintered at (d) 750^{o}C, (e) 800^{o}C, and (f) 850^{o}C.

Fig. 6 HRTEM image of the Cu-doped $Mg^{11}B_2$ sample sintered at 800^{o}C.

Fig. 7 Temperature dependence of ZFC magnetization for the $Mg^{11}B_2$ and the $Mg^{11}B_2$+5 wt.% Cu samples.

Fig. 8 Measured J_c-H characteristics of the the $Mg^{11}B_2$ samples and the $Mg^{11}B_2$+5 wt.% Cu samples at 20K. The reference MgB_2 is made from normal boron [20].

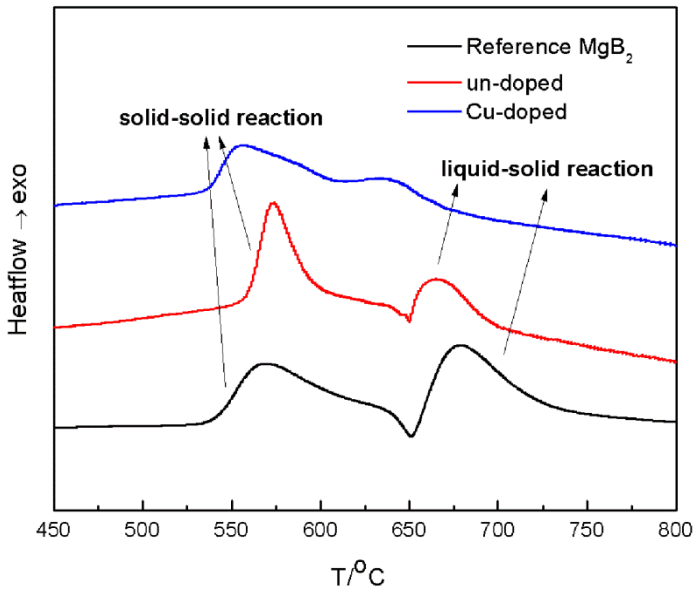
Reference MgB2
un-doped
Cu-doped
solid-solid reaction
liquid-solid reaction
Heatflow → exo
450
500
550
600
650
700
750
800
T/°C

Fig. 1

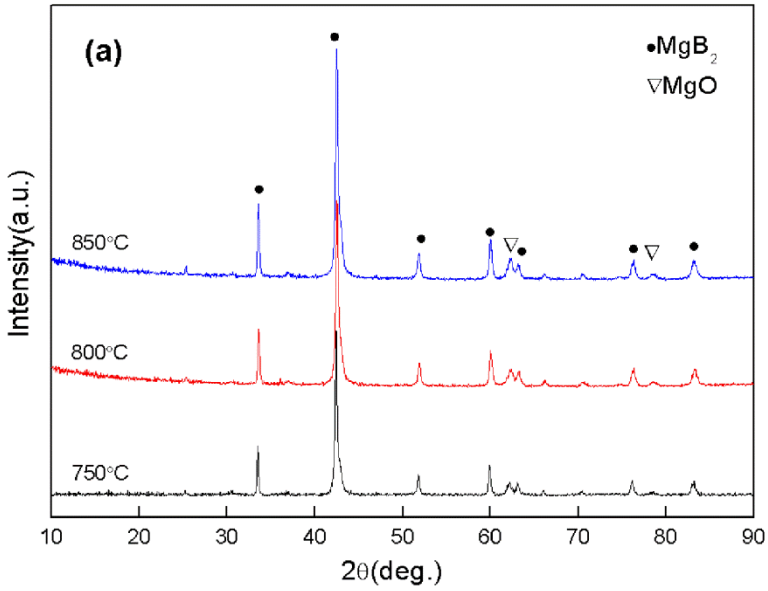
(a)
•MgB2
▽MgO
850°C
800°C
750°C
Intensity(a.u.)
10
20
30
40
50
60
70
80
90
2θ(deg.)

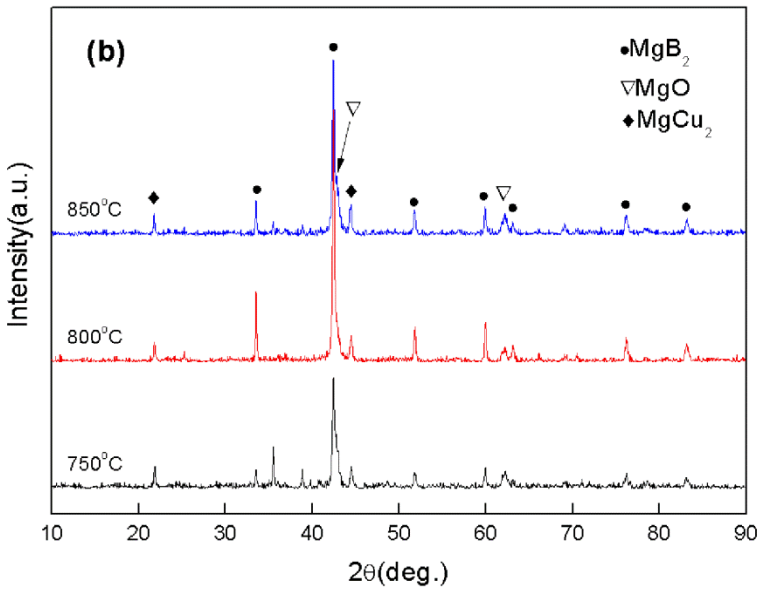
(b)
•MgB2
▽MgO
♦MgCu2
850°C
800°C
750°C
Intensity(a.u.)
10
20
30
40
50
60
70
80
90
2θ(deg.)

Fig. 2

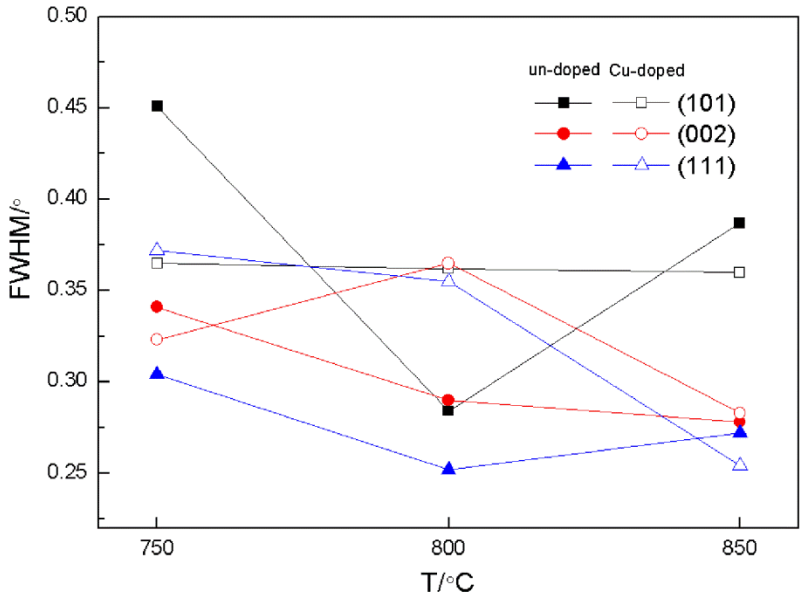
un-doped Cu-doped
(101)
(002)
(111)
FWHM/°
0.50
0.45
0.40
0.35
0.30
0.25
750
800
850
T/°C

Fig. 3

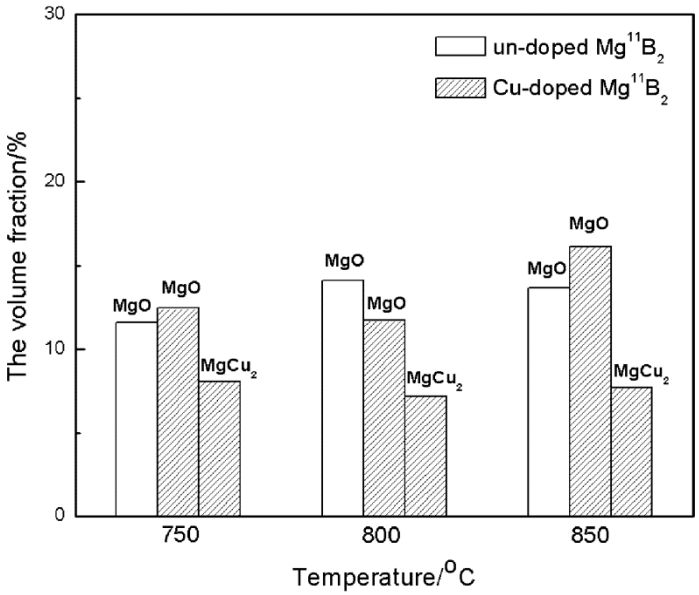
30
20
10
0
The volume fraction/%
un-doped Mg11B2
Cu-doped Mg11B2
MgO
MgO
MgCu2
MgO
MgO
MgCu2
MgO
MgO
MgCu2
750
800
850
Temperature/OC

Fig. 4

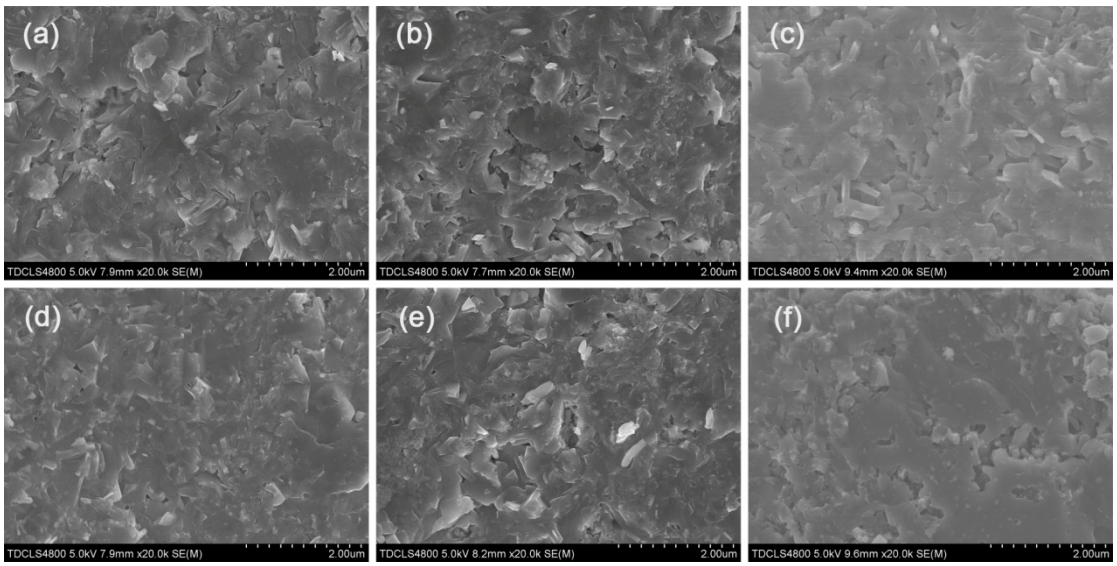
(a)
(b)
(c)
(d)
(e)
(f)
TDCLS4800 5.0kV 7.9mm x20.0k SE(M) 2.00um
TDCLS4800 5.0kV 7.7mm x20.0k SE(M) 2.00um
TDCLS4800 5.0kV 9.4mm x20.0k SE(M) 2.00um
TDCLS4800 5.0kV 7.9mm x20.0k SE(M) 2.00um
TDCLS4800 5.0kV 8.2mm x20.0k SE(M) 2.00um
TDCLS4800 5.0kV 9.6mm x20.0k SE(M) 2.00um

Fig. 5

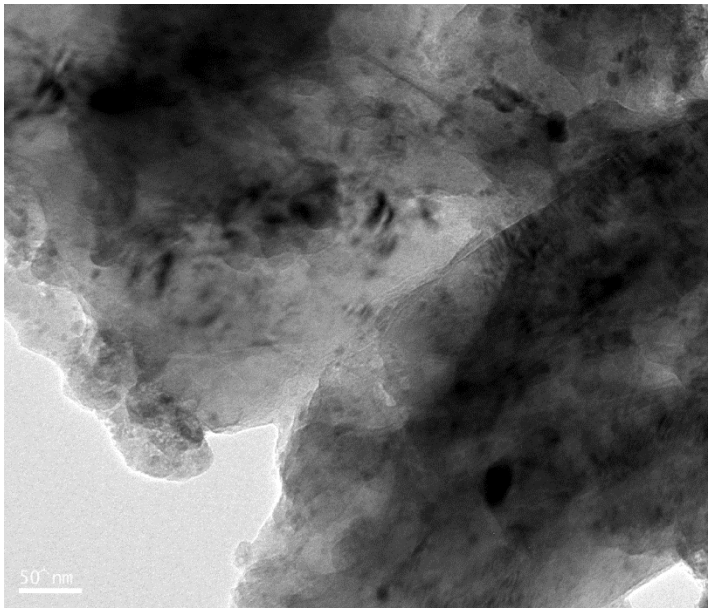
50 nm

Fig. 6

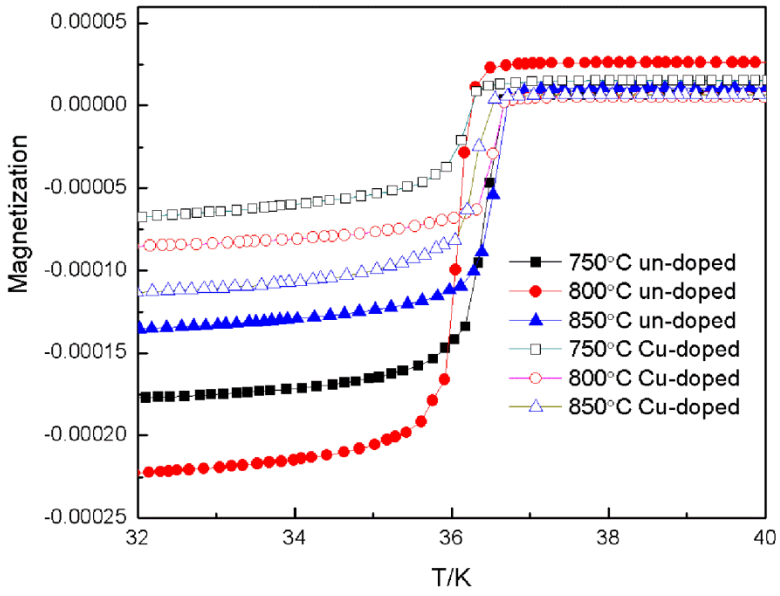
Magnetization
0.00005
0.00000
-0.00005
-0.00010
-0.00015
-0.00020
-0.00025
32
34
36
38
40
T/K
750°C un-doped
800°C un-doped
850°C un-doped
750°C Cu-doped
800°C Cu-doped
850°C Cu-doped

Fig. 7

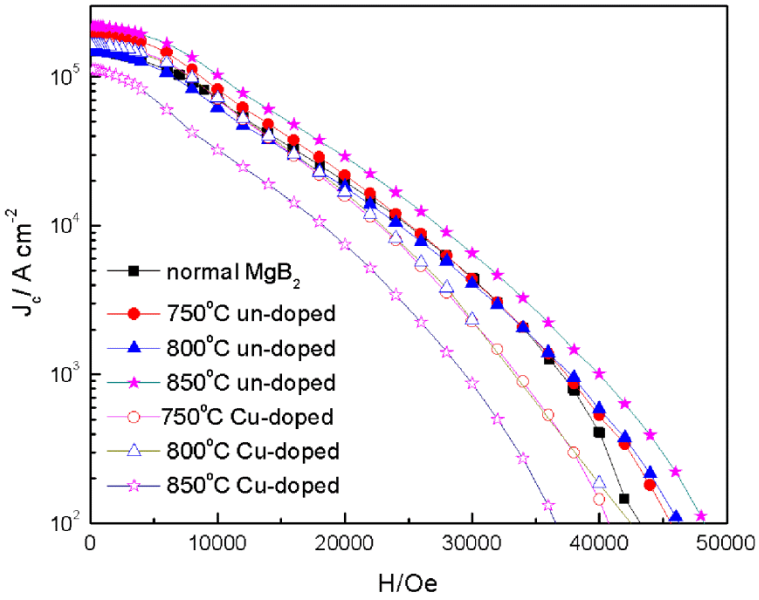
J_c / A cm^{-2}
10^5
10^4
10^3
10^2
0
10000
20000
30000
40000
50000
H/Oe
normal MgB_2
750°C un-doped
800°C un-doped
850°C un-doped
750°C Cu-doped
800°C Cu-doped
850°C Cu-doped

Fig. 8.